Presentation

CURRENT DEVELOPMENTS IN FUTURE PLANETARY PROBE SENSORS FOR TPS: HEATSHIELD ABLATION DETECTOR ADAPTATION TO MID DENSITY ABLATORS

Tomo Oishi [(1)], Ed Martinez [(2)], Johnny Fu [(3)], Sergey Gorbunov [(4)], William Congdon [(5)]

[(1)] ELORET Corporation, MS 231-1, Moffett Field, CA 94035, USA, toihsi@mail.arc.nasa.gov
[(2)] NASA Ames Research Center, MS 229-4, Moffett Field, CA 94035, USA, Ed.Martinez@nasa.gov
[(3)] Sierra Lobo, MS 231-1, Moffett Field, CA 94035, USA, jfu@ mail.arc.nasa.gov
[(4)] ELORET Corporation, MS 229-4, Moffett Field, CA 94035, USA, sgorbunov@mail.arc.nasa.gov
[(5)] ARA Ablatives Laboratory, 14824 E. Hinsdale, Unit C, Centennial, CO 80112, USA, bcongdon@msn.com

ABSTRACT

The NASA Ames version of the Analog Resistance Ablation Detector (ARAD) is tested in Phen-Carb [1] thermal protection system (TPS). The NASA Ames 60 MW arcjet is used to provide the test conditions necessary for significant ablation to evaluate ARAD performance.

1. INTRODUCTION

The ARAD had been successfully used for NASA Jupiter Galileo Mission to monitor entry probe body shape change due to ablation, as part of the atmospheric reconstruction experiment. A few references [2-4] and drawings [5] are available for the Galileo version of ARAD. The recession sensor research capability has been resurrected within NASA to support adaptation to mid density ablators potentially used for planetary exploration probes.

2. ARAD CONSTRUCTION

The Ames ARAD consists of successive layers around a graphite core: 1st Kapton tube; Pt-W wire; 2nd Kapton tube; Ni ribbon; and a 3rd Kapton tube. The schematic of the sensing part and the photograph of the whole Ames ARAD assembly are shown in Fig. 1. The major working parts of the ARAD are the Pt-W resistive wire and the electrically insulating Kapton layers. The Ni ribbon and the graphite core function as internal lead wires. The Kapton gets charred at high temperatures and becomes electrically conductive, making an electrical connection between the graphite core, the Pt-W wire and the Ni ribbon at the location of char. As the charred layer progresses along the axis of the ARAD, the un-charred ARAD length and effective Pt-W wire length decrease, and so does its resistance. The unburned ARAD has electrically conductive epoxy on the tip initially, which functions as a substitute of the charred Kapton, until an actual charred layer forms during its use. The photo of the Ames ARAD shows the entire ARAD assembly including the base section and lead wires. The base section provides transition from fine wires to larger and easier to handle wires.

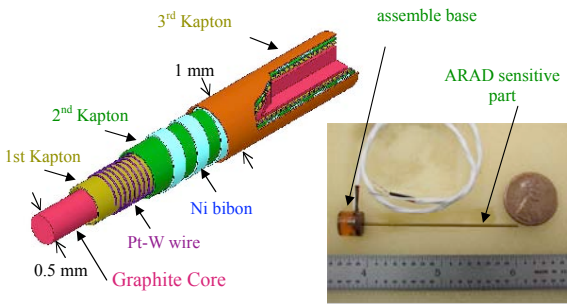

Fig. 1. Ames ARAD schematic

The Ames ARAD design is slightly modified from the Galileo ARAD to simplify fabrication. The difference is a material choice for the core and the shape of the Kapton. For the Galileo ARAD, a Carbon-Phenolic rod (which is the same material as the TPS) was used as a core, while the Ames ARAD currently uses graphite. The core should be made out of the same material as the TPS to minimize intrusiveness by the presence of the ARAD. However, the core needs to be electronically conductive if the measurement scheme used for the Galileo ARAD is followed. For the Galileo ARAD, the core was used as internal lead wires. Intrusiveness consideration was set aside and only the electric conductivity requirement was enforced for the Ames ARAD. Because small diameter carbon-phenolic rods are difficult to obtain, graphite rods were chosen for availability. The Ames ARAD uses tube shaped Kapton, while the Galileo ARAD used Kapton ribbon wrapped with a slight overlap between wraps to form a tube like separation layer. The Kapton tubes make fabrication easier because the wrapping process of the Kapton ribbon, for three layers, is replaced by inserting parts into three different sized Kapton tubes.

Proc. '3rd International Workshop Planetary Probe', Anavyssos, Attiki, Greece, 27 June – 1 July 2005 (ESA SP-607, April 2006)

The ARAD is fit into a hole drilled into the TPS and secured with epoxy. When heat is applied at the surface of the TPS, the TPS ablates together with the ARAD. Below the ablating TPS surface is the charred layer, the pyrorizing layer, and the virgin material. The ARAD outputs the location of the leading boundary of the charred layer, or the boundary between the charred and pyrorizing layers. As the leading boundary of the charred layer advances normal to the ablating surface, the effective length of the ARAD shortens and its output resistance decreases. By monitoring the resistance of the ARAD, its length information is obtained. The ARAD measures the location of the leading boundary of the charred layer or the advance of an isotherm of approximately 700 C, and does not follow the ablating surface directly.

Electronic equivalents of both Galileo and Ames ARAD along with measuring circuits are illustrated in Fig. 2. Since the ARAD changes resistance as its length changes, a measuring system needs to provide excitation to the ARAD. The Galileo ARAD used constant current excitation and the Ames ARAD is operated in the same manner. Although their resistances are much smaller than the Pt-W wire, all elements, whose resistances change proportionally to the ARAD length, are illustrated as potentiometers. The resistance of the Kapton char depends on how it is formed and how intact the charred layer is, therefore, the resistance of the Kapton char is variable. However, in Fig. 2, it is illustrated as a constant resistance element to emphasize non-proportionality to the ARAD length. The Galileo ARAD was operated in a three-legged configuration to remove a resistance contribution from the charred Kapton and the Ni-ribbon. In the three-legged configuration, electronics and the ARAD form two loops, in which the Pt-W wire is shared by both loops. One loop provides current through the Pt-W wire and another loop is used to sense the voltage drop across the Pt-W wire. Since no current flows in the sensing loop, the measured voltage does not contain the voltage drop due to the charred Kapton nor the core. Though it was designed for the three-legged configuration, the Galileo ARAD can be operated in a two-legged configuration by ignoring the Carbon-Phenol core and connecting the negative side of voltmeter to the Ni ribbon. However, operating in the two-legged configuration introduces an error because the measured voltage now contains the voltage drop across the charred Kapton and the Ni ribbon. The Ames ARAD is operated with a flipped three-legged configuration, in which excitation and measurement loops are flipped compared to the Galileo ARAD connection. An extra voltage measurement channel is for diagnostic purposes. The additional channel measures the voltage drop of the two-legged configuration. The difference of two channels, which is the difference between the two and three-legged configuration, is the error introduced by the resistance of the charred Kapton and the graphite core. The magnitude of the error quantifies the importance of the three-legged configuration over two-legged one.

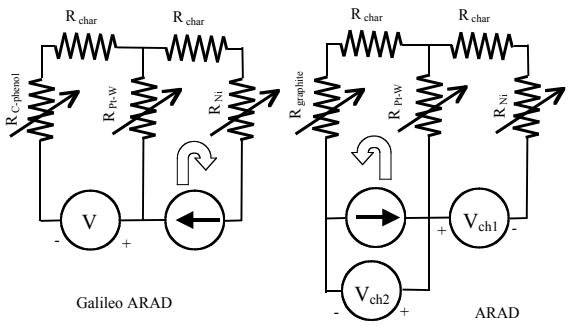

Fig. 2. Electronic schematics for Galileo ARAD and Ames ARAD

3. EXPERIMENTS

Three pairs of Ames ARADs were instrumented in three arcjet test models of different density Phen-Carb TPS. The model is a 76.2 mm diameter cylinder with a convex surface. The cross sectional view of the model is illustrated in Fig. 3. The model has 38.1 mm thick Phen-Carb at the center axis. A pair of Ames ARADs, whose sensing length is 33 mm, were imbedded in Phen-Carb offset 12.7 mm from the center axis of the model. Due to the curvature of the model face, the Ames ARAD tip is 3.2 mm below the surface. Below the Phen-Carb are two layers of cork for insulation and an aluminum base plate for mounting. Lead wires are guided within a bore through the corks and the aluminum. The models are mounted to water-cooled arcjet sting arms at the aluminum plate. The arms position the models in and out of the arcjet flow.

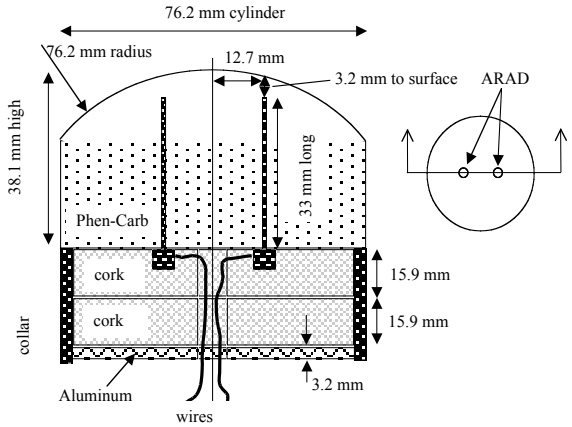

Fig. 3. Cross sectional view of Phen-Carb model

The instrumented models with Ames ARADs were exposed to high convective heating in IHF (Interaction Heating Facility) at NASA Ames. The model density and cold wall heat flux conditions are summarized in Table 1.

Table 1. Arcjet condition for Phen-Carb models

Model#	Density (lb/ft^3)	Density (g/cm^3)	Heat Flux (W/cm^2)	Duration (sec)
PC24	24	0.385	610	45
PC28	28	0.449	835	45
PC32	32	0.513	1003	45

For a constant current excitation, a Lakeshore Model 102 current source set at 1 mA was used for each Ames ARAD. Voltages of Ames ARADs are measured with a KineticSystems CAMAC 3516 DAS system sampling at 3 Hz per channel.

4. RESULTS

As typical results, the raw Ames ARAD reading, the processed length, and the measured char resistance as function of time are plotted in Fig. 4 through Fig. 6 for Phen-carb 24 model (Model PC24). The raw voltage Ames ARAD reading in mV is equal to the resistance of the Ames ARAD in Ω because the constant current is set to 1 mA.

Fig. 4 shows the resistance readings of the Ames ARADs in Model PC24. Soon after the model is inserted to the arcjet stream, the resistance increases slightly, then starts decreasing. This behavior is also observed for the other four Ames ARADs. Fig. 4 shows that both ARADs lost internal contacts at several instances evidenced by large spikes reaching toward zero Ω. ARAD A lost internal contact permanently at 26 sec.

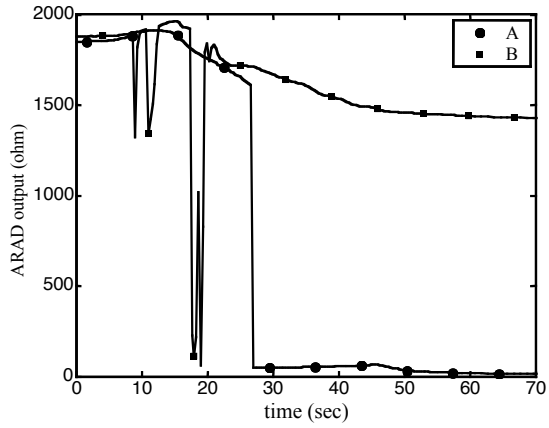

Fig. 4. Raw resistance of Ames ARADs for Model PC24

Fig. 5 shows the location of the tip of the Ames ARADs measured from the original surface of Model PC24 using raw and adjusted data. The length labeled "raw" has a dip which implies an elongation. The dip is the result of the initial resistance increase as seen in Fig. 4. It is possible that the Ames ARAD length actually increases due to thermal expansion of the Ames ARAD itself or the surrounding TPS. However, only a small portion of the Ames ARAD is at a high temperature and TCE (Thermal Coefficient of Expansion) is of tens of ppm in general. It is unlikely to obtain a resistance increase of a few percent due to thermal elongation alone. It is reasonable to assume that no significant thermal elongation occurs and the resistance increase is due to other thermal effects. Further assuming that the temperature distribution in the Ames ARAD is self-similar once the charred layer reaches the tip, then the maximum resistance becomes the resistance of the Ames ARAD at the original length with the included thermal effect. Using the maximum resistance as the base value and treating the resistance change prior to the maximum as the thermal effect, the length is recalculated and plotted as 'adjusted' in Fig. 5.

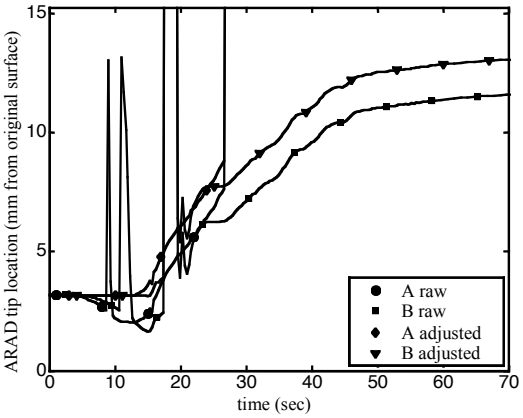

Fig. 5. Raw and adjusted ARAD lengths for Model PC24

One probable cause for the resistance increase is due to a resistivity increase of the Pt-W wire with temperature. Although its TCR (Temperature Coefficient of Resistivity) is on the order of magnitude smaller than pure platinum, the Pt-W wire has non negligible TCR of 250 ppm [6]. The value is large enough to provide a few percent of resistance increase with reasonable temperature distribution within the Ames ARAD.

Another possibility for resistance increase is that the resistance increase did not originate from the Pt-W wire resistance but is an error due to thermoelectric voltage. The ARAD is made out of different materials. The Channel 1 measurement path in Fig. 2 consists of the Pt-W wire, the charred Kapton and the Ni ribbon. They form a Pt-W and Ni thermocouple with an ambiguous thermocouple junction because of the charred layer. The thermoelectric voltage is added to the voltage drop across the Pt-W wire. Originally this possibility is discarded because of 70 to 90 Ω increases in Fig. 4, which corresponds to 70 to 90 mV. The value of 70 mV is almost the same as Type E thermocouple output at 1000 C, which is the most sensitive one among letter designated thermocouples, and 70 mV is much larger than the output of letter-designated platinum based thermocouples of 20 mV at 1700 C. Originally, it was believed that a non-letter designated thermocouple can only produce a few millivolts at mere 700 C. A Pt-W and Ni thermocouple was constructed and tested for thermoelectric voltage to isolate and bound this effect. It produces 23 mV at 700 C with a room temperature cold junction. Although the thermoelectric voltage is not as large as the whole change of 70 mV, it is not negligible either.

One other possible cause of the resistance increase is a TCE mismatch. If the Pt-W wire is restricted from moving freely, it is strained and its resistivity changes due to this strain. The strain gage factor of the Pt-W is 3.8 [6]. To produce resistivity differences in the same magnitude as the TCR, the TCE mismatch has to be one hundred ppm. If the TCE of the graphite core is as small as other common material, the resistivity change is dominated by the TCR.

The initial resistance increase is more likely to be the result of the sum of the causes mentioned above.

The extra channels recorded the resistance of the current excitation path, which consists of the graphite core, the Kapton Char and the Pt-W wire. The Ames ARAD output, the resistance of the Pt-W alone, is already shown in Fig. 4. Subtracting the Pt-W resistance from the resistance of the current excitation path provides the resistance of the graphite core and the charred Kapton, which is plotted in Fig. 6. The resistance of the graphite core at the room temperature of the unburned length is 2 Ω. Even with resistance increases of the graphite core due to the TCR, the graphite core resistance is bounded within a few ohms. Therefore, the resistance difference plotted in Fig. 6 is mostly from the Kapton char. However, the negative value of Fig. 6 implies that there is a definite thermoelectric effect. It should be emphasized that Fig. 6 shows the "measured" Kapton Char resistance with a very large uncertainty due to thermoelectric effects. In the least, Fig. 6 is useful as visualization of the error if the two-legged configuration had been used instead of the three-legged configuration. Compared to the initial resistance increases shown in Fig. 4, the uncertainty due to the Kapton char resistance is smaller. In the current Ames ARAD design, a resistance uncertainty of 50 Ω corresponds to 0.9 mm error. If this magnitude of a measurement error is tolerable for an application, there is no need to operate the ARAD in the three-legged configuration. The two-legged configuration relaxes the design requirements of future ARADs. Any TPS material can be the ARAD core or the Ni ribbon can be removed if the TPS core is conductive, such as the Carbon-Phenol.

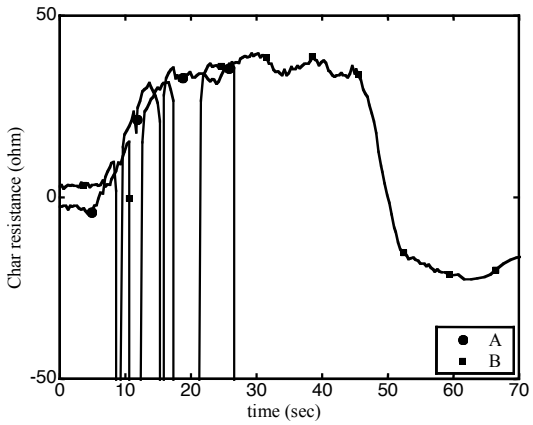

Fig. 6. Char resistance for Model PC24

The adjusted Ames ARAD experimental data is compared to numerical solutions in Fig. 7 and Fig. 8. Numerical material response simulation is performed for Model PC24 and PC28 with heat fluxes given in Table 1. The location of the 700 C node is plotted as function of time along with "adjusted" Ames ARAD data. The numerical isotherm of Model PC32 is not available, and only experimental data is shown in Fig. 9.

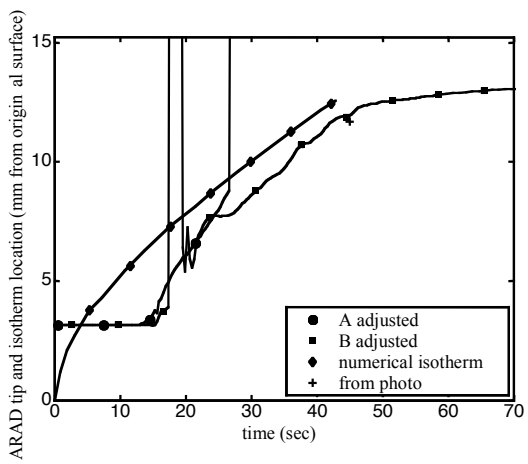

Fig. 7. Comparison of Ames ARAD measurement to numerical isotherm prediction for Model PC24

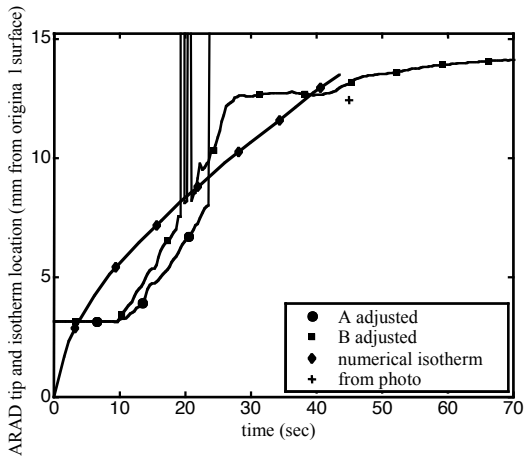

Fig. 8. Comparison of Ames ARAD measurement to numerical isotherm prediction for Model PC28

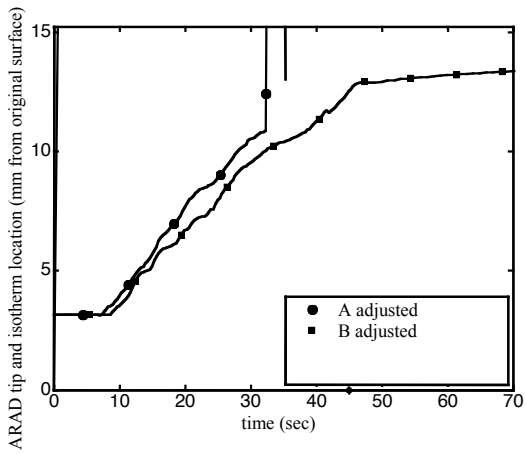

Fig. 9. Ames ARAD measurement for Model PC32

Postmortem analysis is performed by cross sectioning the models and taking photographs. Assuming the TPS response is frozen when the model is taken out of the arcjet flow, one more data point can be obtained from the photo. As shown in Fig. 10 and Fig. 11, the tip of the advancing charred layer can be determined visually from the photos. The result from the photo analysis is plotted as single point at 45 sec in Fig. 7 and Fig. 8.

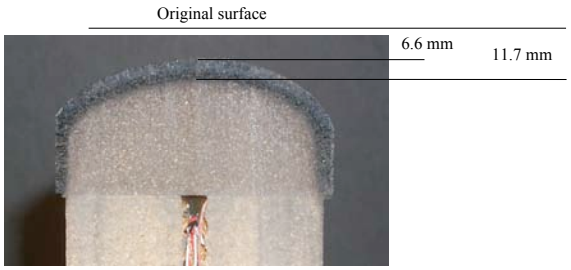

Fig. 10. Cross sectional photograph of Model PC24

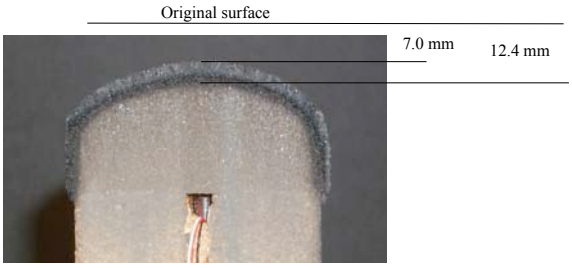

Fig. 11. Cross sectional photograph of Model PC28

5. FUTURE WORK

More fundamental experiments shall be conducted to determine the cause of the initial resistance increase Some alternate design parameters, sizes of Kapton tubes and wire wrapping strength and direction for example, shall be tried to improve inner electric contacts. To eliminate the concern of the thermoelectric voltage effect to the initial resistance increase issue, the Ni ribbon could be replaced with the Pt-W wire. To reduce the resistance change due to the TCR without compromising other physical parameters, other material candidate should be tried to replace the Pt-W. To minimize the intrusiveness of the ARAD, the core material shall be made out of the same material as the TPS.

6. CONCLUSIONS

These ARAD experiments revealed several issues. Full duration survivability in these material is about 50 %, possibly due to relatively low heating rates seen in these experiments versus Galileo probe heating rates. The raw data indicated initial elongation in an unrealistic magnitude. A simple adjustment is applied to correct the elongation issue. However, the sensor has shown that an active measurement of an ~700 C isotherm recession rate and location can be traced in a ground based verification type test. This leads to the strong capability to fly an ARAD recession sensor to provide ground to flight verification of TPS aerothermal design tools – leading directly to risk quantification and risk reduction.

7. REFERENCES

1. Laub, B., Chen, Y., TPS Challenges for Neptune Aerocapture, AIAA Atmospheric Flight Mechanics Conference and Exhibit, RI, Aug 16-19, 2004
2. Cassanto, J. M., Droms, C. R., Metzger, J., A Simple Recession Gage for Inflight Measurement of the Char Degradation Zone for Re-Entry Vehicle Heatshield, 26th International Instrumentation Symposium, Seattle, Washington, May, 1980
3. Milos, F. S., Galileo Probe Heat Shield Ablation Experiment, *Journal of Spacecraft and Rockets*, Vol. 34, No. 6, 1997, pp. 705-713
4. Milos, F. S., Chen, Y-K., Squire, T. H., Analysis of Galileo Probe Heatshield Ablation and Temperature Data, *Journal of Spacecraft and Rockets*, Vol. 36, No. 3, 1997, pp. 298-305
5. Analog Resistance Ablation Detector (ARAD), Re-Entry Systems Operations, General Electric Co., Contract 08-737444-LD4, Drawing 47D523037, Rev. B, Philadelphia, Pa, Aug. 1979
6. Bertodo, R., Precious Metal Alloys for High Temperature Resistance Strain Gauges, *Journal of Physics D*, 1968, Series 2, Vol. 1